Supplementary Materials

Collagen Nanobubbles as Efficient Carriers for Targeted Controlled Release of Ibrutinib

Sena Pişkin[1], Handan Sevim Akan[2], Canan Armutcu[1], Lokman Uzun[1*]

[1]Hacettepe University, Faculty of Science, Department of Chemistry, Ankara, Turkiye

[2]Hacettepe University, Faculty of Science, Department of Biology, Ankara, Turkiye

[*]Corresponding author: Address: L. Uzun, Prof. Dr.; Hacettepe University, Faculty of Science, Department of Chemistry, Biochemistry Division, 06800-Beytepe, Ankara-Turkiye. Email: lokman@hacettepe.edu.tr; Tel: +90312 297 7337

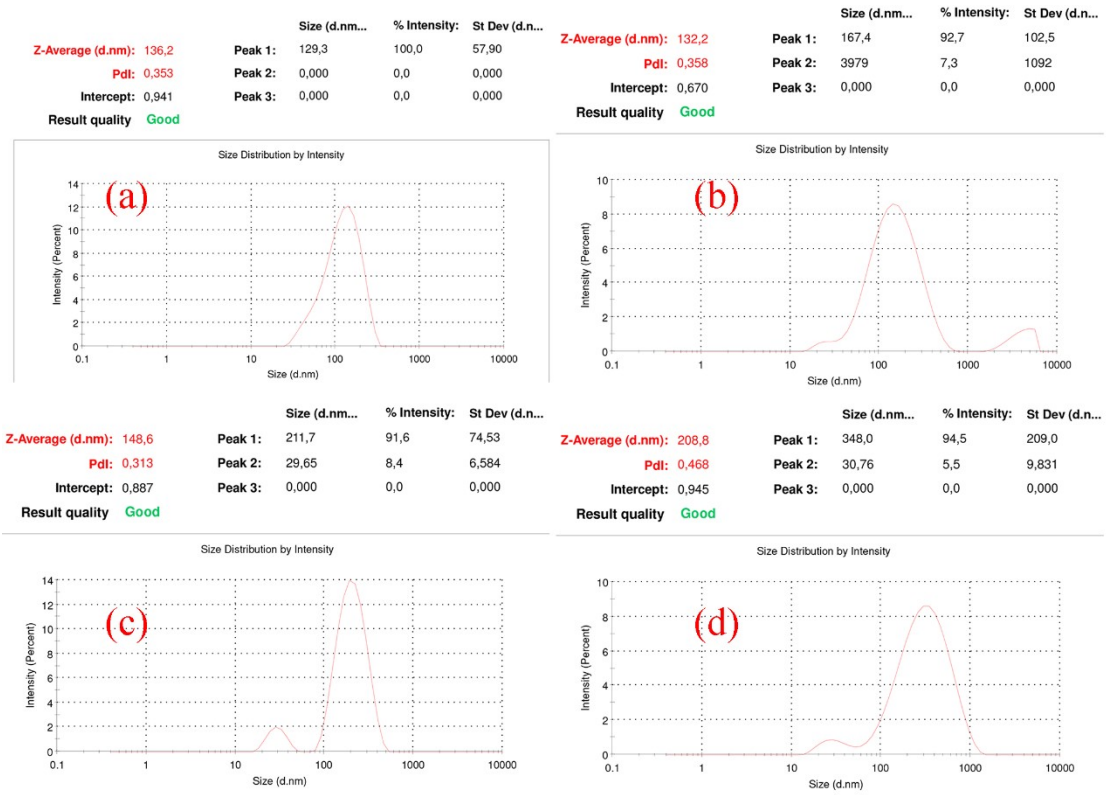

Figure S1. Zeta-size measurements for the nanobubbles: (a) 1 mg-, (b) 2 mg-, (c) 3 mg-, and (d) 4 mg-drug loaded nanobubbles.

Stability of Nanobubbles

While there is no universally accepted theory of NB stability, Laplace pressure (ΔP) indicates that bubble stability decreases with bubble radius (r) ($\Delta P=-2\sigma/r$, where σ (sigma) is the surface tension).[1] This indicates that NBs coalesce and are no longer in the measurable size range. Many studies have incorporated combinations of nonionic poloxamers[2], cross-linked polymers[3] and anionic lipids[4,5] into their shells to extend the lifetime of NBs. Traditionally, these approaches have been aimed at inhibiting dissolution by reducing surface tension or reducing bubble coalescence through electrostatic repulsion. In this study, Pluronic F68 solution was added to the formulation to improve the physical stability of the bubbles. Pluronic F68 is an amphiphilic, non-

ionic block copolymer composed of ethylene and propylene oxide units widely used in pharmaceuticals. The role of this substance in the formulation is to inhibit the aggregation of NBs through steric stabilization by the dominant solvation effect. When added to the aqueous suspension of nanobubbles, this non-ionic stabilizer adsorbs to the nanobubble shell via the linker segment and the well-solubilized tail segment extends towards the external aqueous environment, preventing particle aggregation.[6] On the other hand, nanobubble formation process was performed in ice-bath to inhibit vapor pressure of the filling gas, in other word, to improve the nanobubble stability. In order to confirm the presence of gaseous-filler in the core of nanobubbles, we have conducted a set of experiment including pure perfluoropentane (PFP), nanobubble dispersion before and after explosion process (**Figure S2**). Herein, gas chromatography/mass spectrometry measurements were performed under the conditions summarized in the **Table S1**. As seen in the **Figure S3**, pure PFP sample has a single peak in the chromatogram and different peaks in mass/charge spectrum those revealed out the cracking, coupling, and replacement reactions were occurred during the analysis process. Before explosion process (**Figure S4**), although there is a single peak in the chromatogram as well, it is not related to the filling gas, PFP because the mass spectra have no related mass/charge peaks observed in the pure PFP sample. These peaks mostly related to the organic solvent (especially ethanol) and other volatile species in the media. Whenever the results (**Figure S5**) obtained from the samples after explosion with not only ultrasonication but also heating to 33^{o}C (5^{o}C higher than boiling point of PFP) to boost out the all PFP molecules into gaseous phase, the similar

chromatogram was obtained with pure PFP sample except extra a second peak which was related to the solvent as observed in sample 2. The mass spectra were also well-matched with those obtained from previous samples. The results confirmed that the some of PFP molecules presented in the core of nanobubbles as well as being released after explosion as expected. According to the new results besides the presence of amphiphilic agents, it should be concluded that the PFP molecules were stabilized and stacked into the core of the nanobubbles. Moreover, although the formulation looks like double-emulsion system, the nanobubbles were formed via a competitive dissolution/aggregation process.

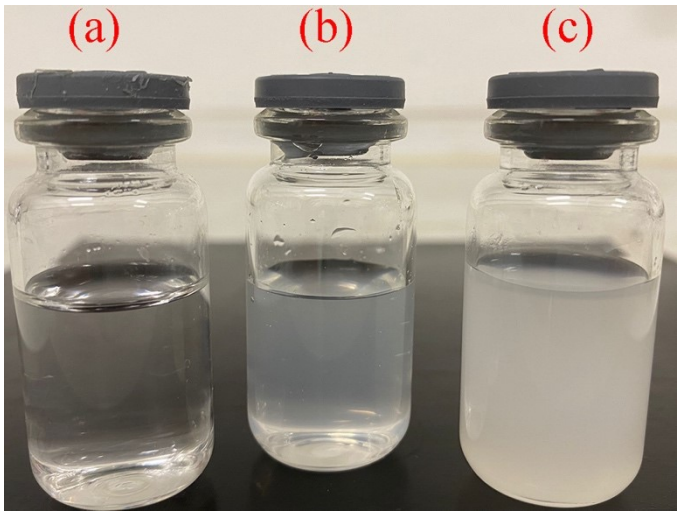

Figure S2. Optical images of samples including (a) free perfluoropentane and nanobubbles (b) before, and (c) after ultrasound treatment.

Table S1. Summary of the conditions for Gas chromatography-mass spectrometry (GC-MS) analysis.

Column Oven Temp.	30˚C	**Ion Source**	200
Injection Temp.	260˚C	**Interphase temp.**	280
Injection Mode	Split (1/10)	**Solvent Cut Time**	0.5 min
Carrier Gas	Helium (1 mL/min)		
Rate	**Final Temperature (˚C)**	**Hold Time (min)**	
-	30	3.0	
10	200	2.0	
20	310	10	
Column (Rxi-5HT)	Length: 30.0 m	Thickness: 0.25 µm	Diameter: 0.25 mm

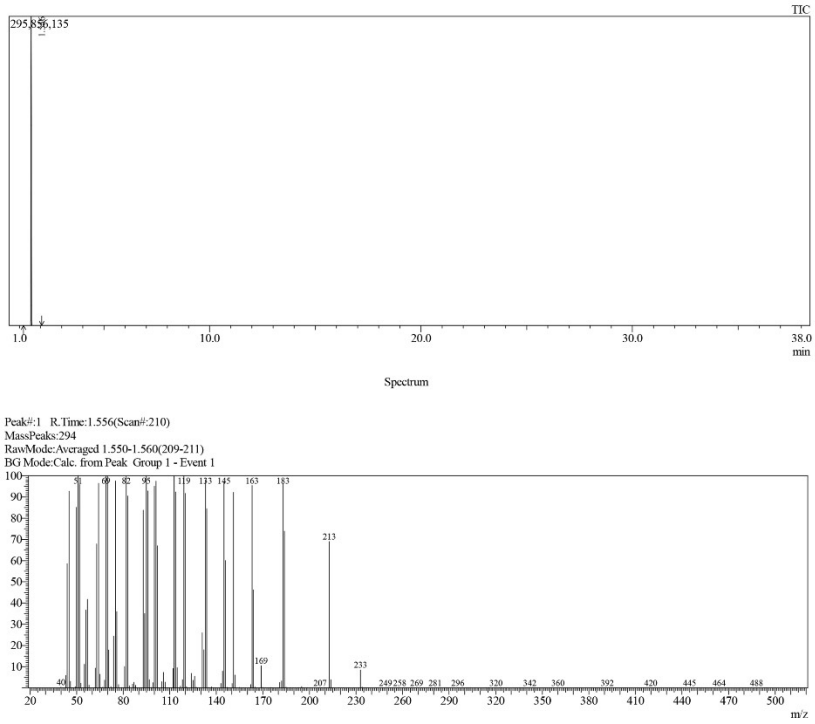

Figure S3. Gas chromatography-mass spectrometry analysis of pure perfluoropentane.

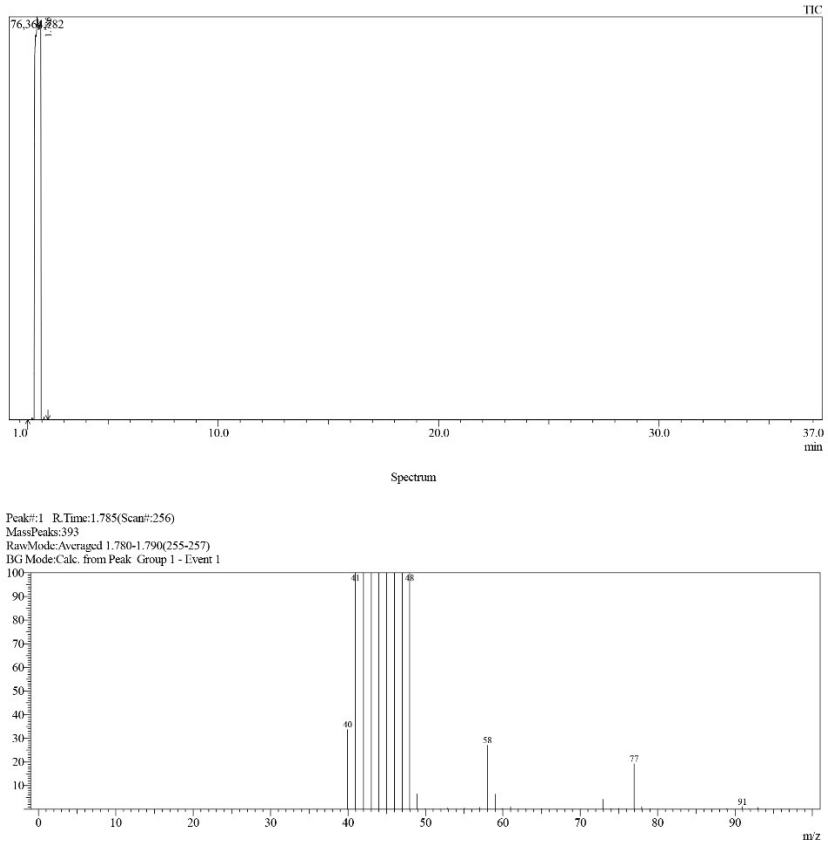

Figure S4. Gas chromatography-mass spectrometry analysis of nanobubble dispersion before ultrasound treatment.

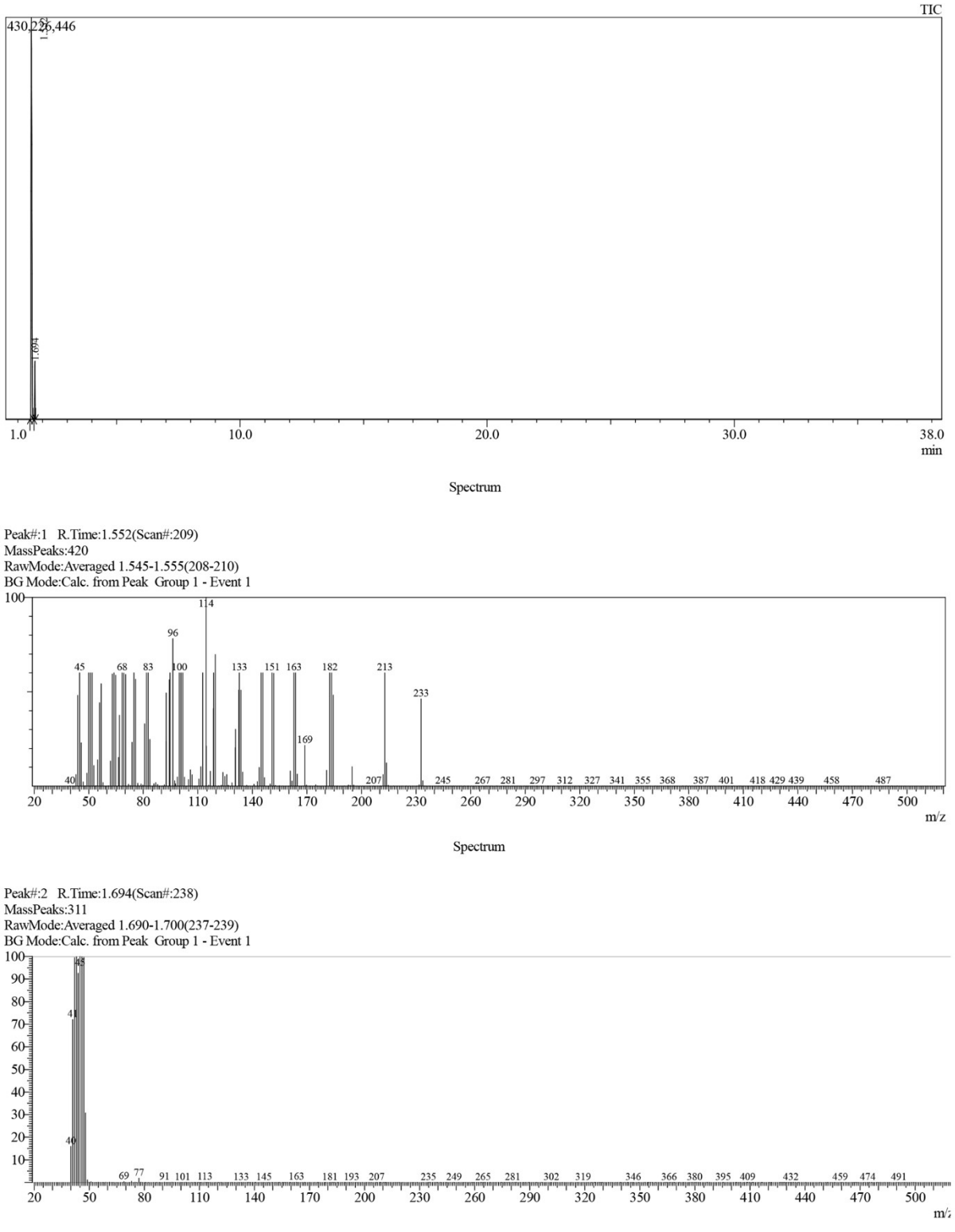

Figure S5. Gas chromatography-mass spectrometry analysis of nanobubble dispersion after ultrasound treatment.

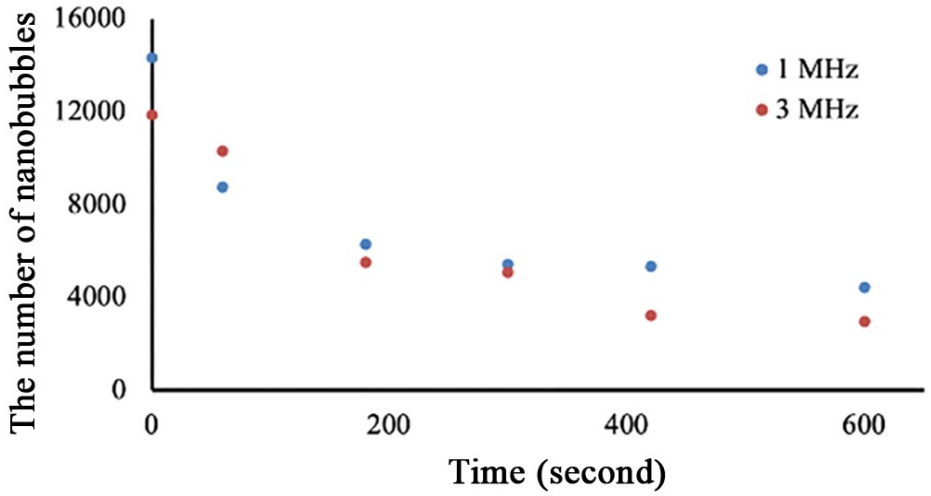

Figure S6. The effects of ultrasound power density and treatment duration on the nanobubbles.

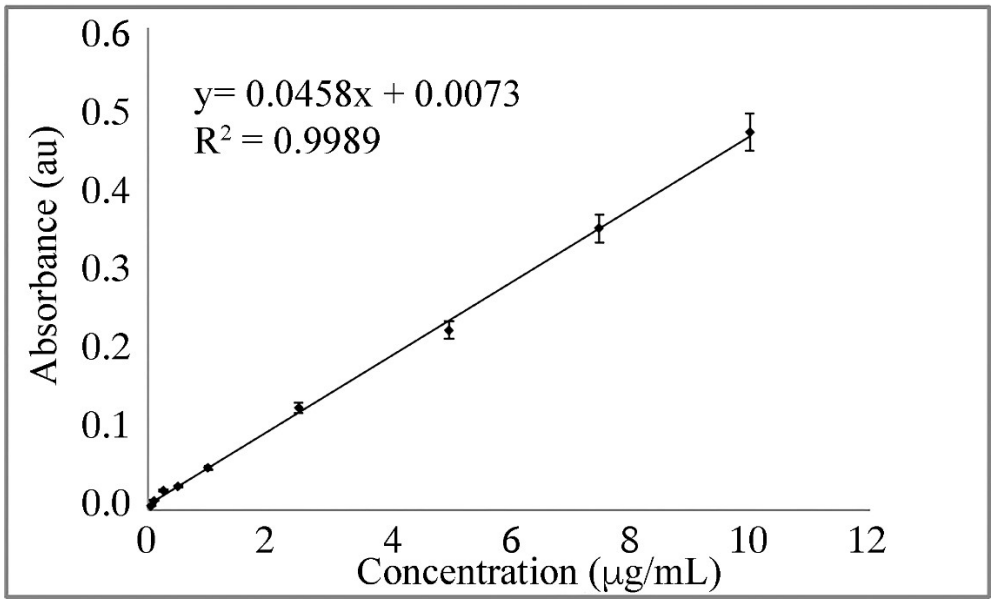

Figure S7. Calibration curve of IBR solution

Release kinetics studies from nanobubbles

without ultrasound treatment at pH 7.4

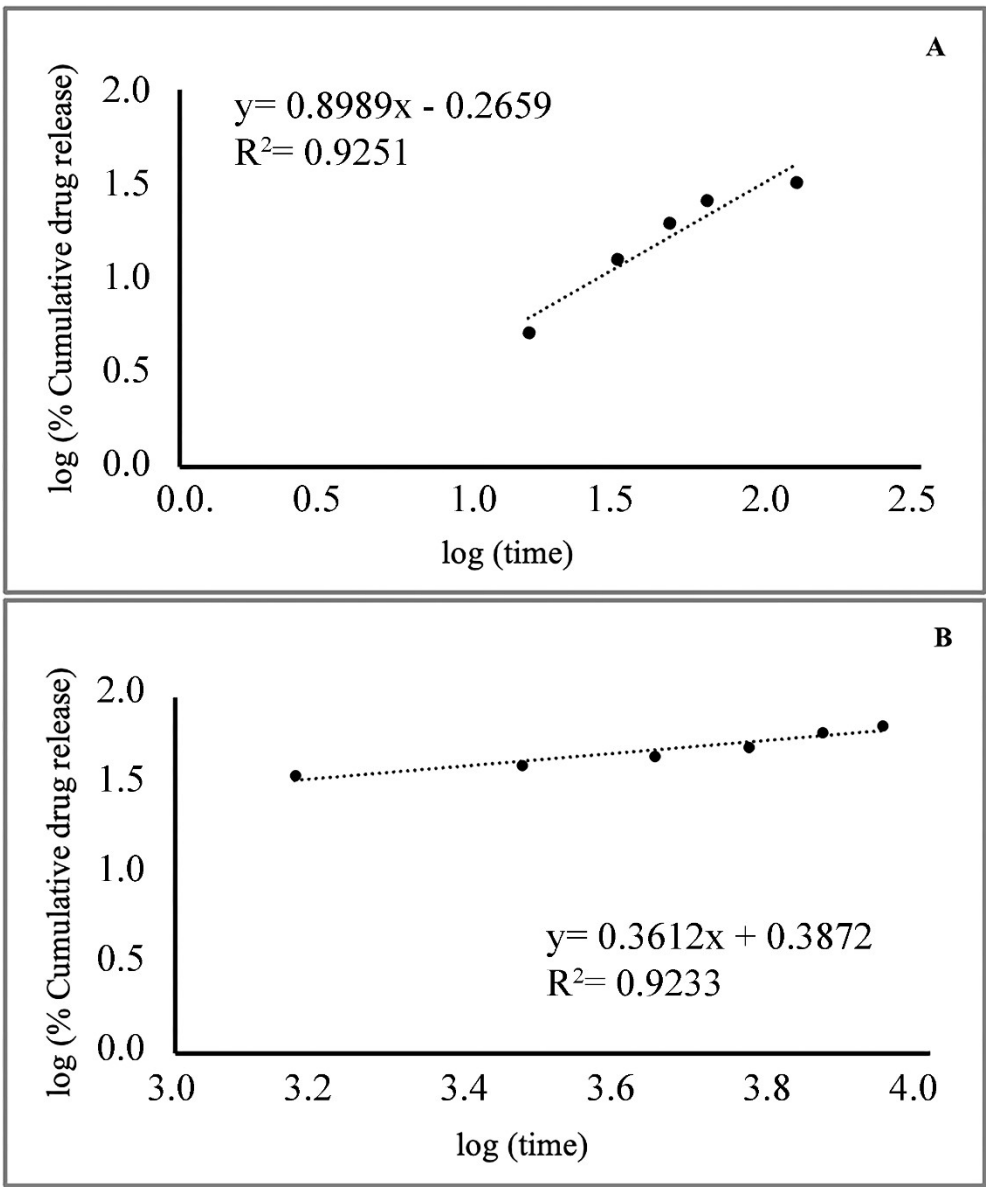

Figure S8. Korsmeyer-Peppas model for releasing kinetics without ultrasound treatment at pH: 7.4 for (A) the first 120 min and (B) further time intervals up to 6 days (1440-8640 min).

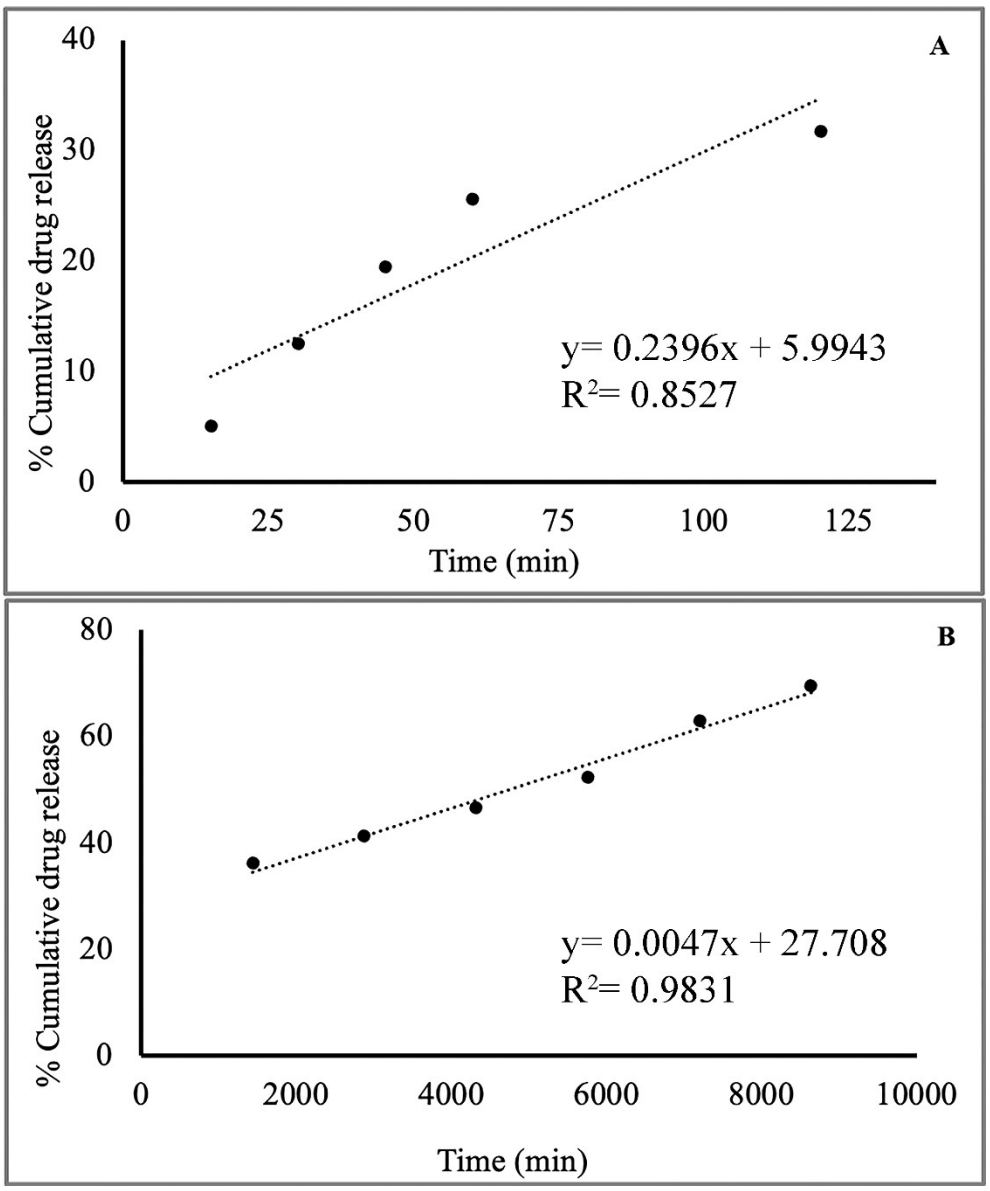

Figure S9. Zeroth-order kinetic model for releasing kinetics without ultrasound treatment at pH: 7.4 for (A) the first 120 min and (B) further time intervals up to 6 days (1440-8640 min).

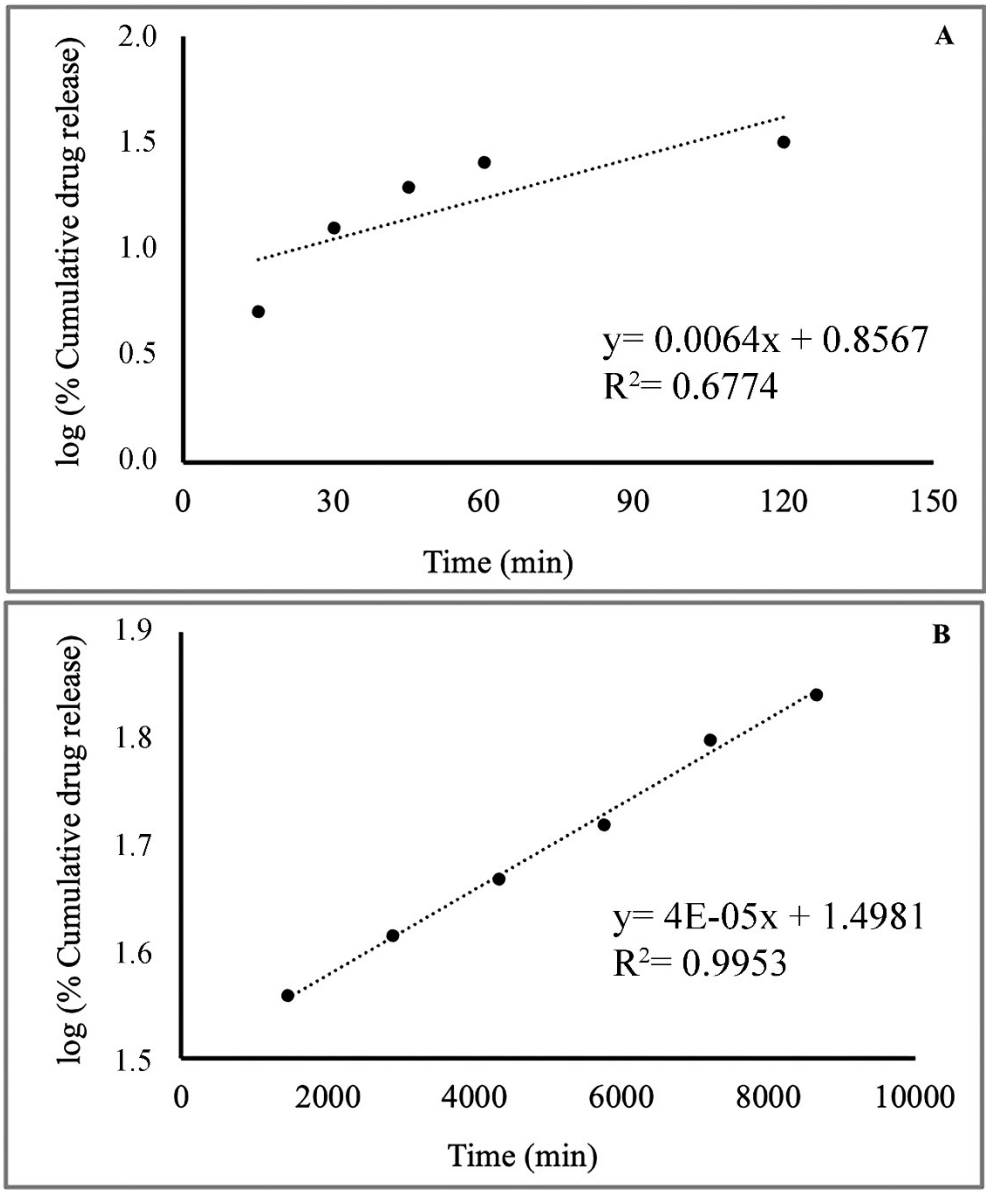

Figure S10. First-order kinetic model for releasing kinetics without ultrasound treatment at pH: 7.4 for (A) the first 120 min and (B) further time intervals up to 6 days (1440-8640 min).

Release kinetics studies from nanobubbles with ultrasound treatment at pH 7.4

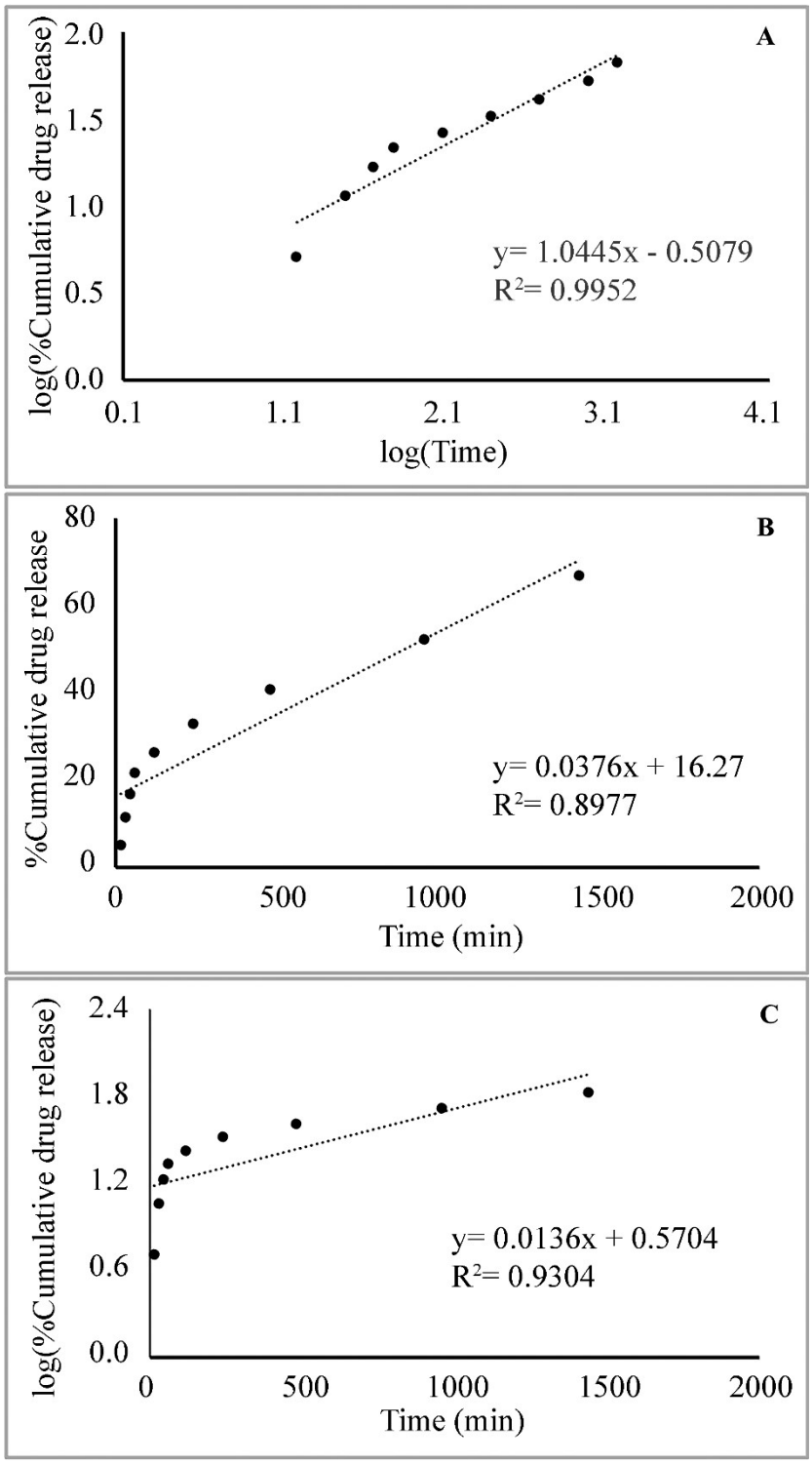

Figure S11. The releasing kinetics with ultrasound treatment at pH: 7.4 for 24 hours. (A) Korsmeyer-Peppas, (B) Zeroth-order, and (C) First-order release kinetic models.

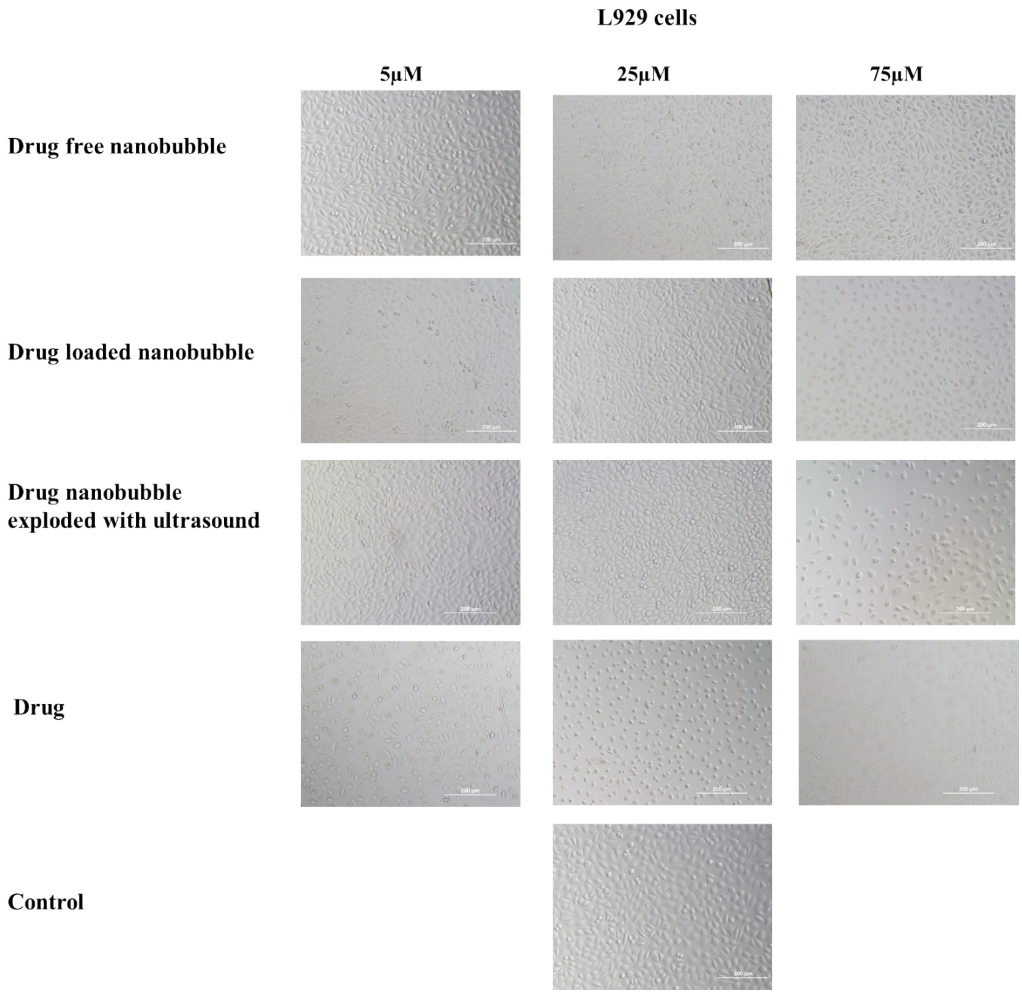

Figure S12. Morphological changes of L929 cells after treatment with drug-free, drug-loaded, ultrasound-exploded nanobubbles, and free drug at different concentrations for 24 hours. Epithelial-like morphology was preserved in the control group and drug-free nanobubble group whereas a major change in the morphology of the cells was observed in drug-loaded, ultrasound-exploded nanobubbles, and free drug groups 25 µM concentration (10X magnification, DP71; Olympus, Tokyo, Japan).

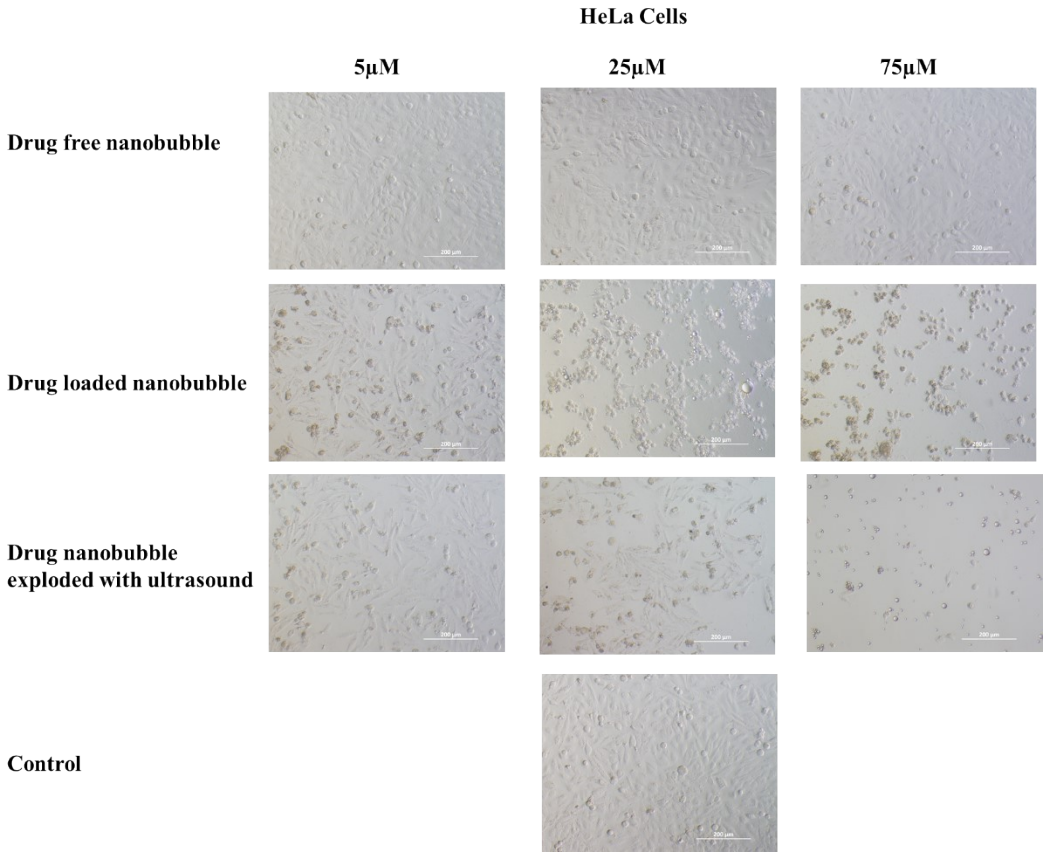

Figure S13. Morphological changes of HeLa cells after treatment with drug-free, drug-loaded, ultrasound-exploded nanobubbles at different concentrations for 24 hours. The free drug group caused excessive cell death for HeLa cells; therefore, the morphology of the cells was not shown. Epithelial-like morphology was preserved in the control group and drug-free nanobubble group whereas a significant change in the morphology of the cells was observed in drug-loaded, ultrasound-exploded nanobubbles, and free drug groups starting with 5 µM concentration (10X magnification, DP71; Olympus, Tokyo, Japan).

References

1. D. V. Batchelor, F. J. Armistead, N. Ingram, S. A. Peyman, J. R. Mclaughlan, P. L. Coletta And S. D. Evans, Langmuir, 2022, 38, 13943-13954.
2. H. Wu, E.C. Abenojar, R. Perera, T. An, A.A. Exner, Ultrasound In Medicine &

Biology, 2019, 45(9), 2502-2514.

3. P. Nittayacharn, H.-X. Yuan, C. Hernandez, P. Bielecki, H. Zhou, A.A. Exner, Journal Of Pharmaceutical Sciences, 2019, 108, 3091-3098.
4. T. Yin, P. Wang, R. Zheng, B. Zheng, D. Cheng, X. Zhang, X. Shuai, International Journal Of Nanomedicine, 2012, 7, 895-904.
5. R.H. Perera, H. Wu, P. Peiris, C. Hernandez, A. Burke, H. Zhang, A.A. Exner, Nanomedicine: Nanotechnology, Biology And Medicine, 2017, 13(1), 59-67.
6. R. Cavalli, M. Argenziano, E. Vigna, P. Giustetto, E. Torres, S. Aime, E. Terreno, Colloids And Surfaces B: Biointerfaces, 2015, 129, 39-46.